The Carnegie Planet Finder Spectrograph

Jeffrey D. Crane[a], Stephen A. Shectman[a] and R. Paul Butler[b]

[a]Observatories of the Carnegie Institution of Washington,
813 Santa Barbara Street, Pasadena, CA, USA 91101;
[b]Department of Terrestrial Magnetism, Carnegie Institution of Washington,
5241 Broad Branch Road, NW, Washington, DC, USA 20015

ABSTRACT

The Carnegie Planet Finder Spectrograph is being constructed for use at the Magellan Telescopes at Las Campanas Observatory in Chile. Its primary scientific objective is the detection of extrasolar planets through monitoring of stellar radial velocity variations. The spectrograph is being optimized for high precision measurement of these velocities with a resolution goal of 1 m s^{-1}. The optical design includes all spherical, standard optical glass and calcium fluoride lenses that function as both camera and collimator in a double-pass configuration. A prism cross-disperser is also used in double-pass and provides a minimum order separation of 4.0 arcsec. An R4 echelle grating is illuminated near true Littrow and provides complete wavelength coverage between 390 nm and 620 nm. Spectral resolution is 38,000 when using a 1 arcsec slit, although slit widths as small as 0.2 arcsec are available. An iodine cell is used to superimpose well-defined absorption features onto spectra to serve as a fiducial wavelength scale, and a thorium argon lamp is available for traditional wavelength calibrations. The spectrograph is currently under construction and is scheduled for commissioning in the second quarter of 2007.

Keywords: spectrograph, spectroscopy, echelle, high resolution, radial velocity, extrasolar planet

1. OVERVIEW AND DESIGN GOALS

The definition and constraint of planetary formation models will benefit from the development of a large, statistically significant and unbiased catalogue of extrasolar planetary systems. Extrasolar planetary searches often employ the method of monitoring stellar radial velocities to look for periodic variations that may indicate the presence of a gravitationally influential orbiting mass. At first, such searches are naturally biased toward detecting massive planets at small orbital radii. However, long-term monitoring of a large sample of potential planetary host stars will increase detection sensitivity to planets orbiting at larger radii. Furthermore, improving the *precision* of radial velocity measurements will increase the survey sensitivity to planets both with larger orbital radii and smaller masses.

The motivation for the Carnegie Planet Finder Spectrograph (PFS) is to enable a long-term observing program at Las Campanas Observatory (LCO) capable of monitoring the radial velocities of about 1000 late-type stars with a precision of 1 m s^{-1}. The instrument will be used with the 6.5m Landon Clay (Magellan II) telescope. The PFS will be positioned at the nasmyth focus when in use and moved to a storage area when not in use.

There are a number of deleterious instrumental effects that can limit the accuracy of radial velocity measurements. The design of the PFS is motivated by the desire to minimize these effects while maintaining relative simplicity and low cost. Thermal and mechanical stability are important, as are even illumination of the pupil and image planes and detailed intensity calibration at the detector.

The PFS will use an iodine cell[1] to imprint known spectral absorption features on each stellar spectrum. This method is highly effective at removing most deleterious instrumental effects since the stellar and reference spectra are collected simultaneously over exactly the same instrumental optical path. The goal for PFS is therefore not

Further author information:
J.D.C.: E-mail: crane@ociw.edu, Telephone: 1 626 304 0217
S.A.S.: E-mail: shec@ociw.edu, Telephone: 1 626 304 0219
R.P.B.: E-mail: paul@dtm.ciw.edu, Telephone: 1 202 478 8866

to completely remove all sources of variable instrumental spectral drift, but simply to minimize them as much as possible within the constraints of the budget. If the remaining drifts can be expected to vary smoothly and mildly with time, then any residual effects that are not automatically removed by the iodine cell can be reliably accounted for by interpolative calibration. This is similar to the philosophy employed by UVES[2] at the VLT.

The primary wavelength range of interest is that part of the spectrum blanketed by sufficiently deep iodine absorption features: 5000-6200 Å. In addition, coverage to 3900Å is desired to allow use of the calcium H and K lines to probe stellar atmospheric conditions.

2. OPTICAL DESIGN

A summary of the PFS optical characteristics is given in Table 1, with more information detailed in the following sections.

Table 1. Summary of optical characteristics

Telescope	6.5m aperture, F/11
Guider	1024×1024 EEV CCD, 13μm pixels, 38×38 arcsec FOV
Focal reducer	20mm pupil, F/11 to F/5 conversion
Slit	3.7 arcsec length, 0.2-2.5 arcsec discrete widths available
Collimator/camera	dioptric, F/5, 750mm effective focal length
Disperser	R4 echelle grating, 76° blaze, 154×408 ruled area
Cross-disperser	PBM2 prism, 43° apex angle
Detector	4096×4096 SITe CCD, 15μm pixels
Spectra	3900-6200Å full coverage across 58 orders, R=38000

2.1. Camera

The spectrograph optics are used in double-pass and so act both as collimator and camera. However, these optics will henceforth be referred to as the camera. The optical design of the PFS camera was modeled after the red channel of the MIKE[3] spectrograph at LCO. The optical layout is shown in Figure 1.

The fully dioptric camera is F/5.0 with a 150 mm diameter pupil. The optics are all spherical and are separated into three widely spaced groups effectively in a singlet-triplet-singlet configuration. However, the central calcium fluoride lens of the triplet has been split into two thinner pieces to ease acquisition of the blank material. The remaining elements are standard Ohara glasses. A fused silica field flattener also serves as the CCD dewar window. A matching fused silica lens follows the entrance slit, but has been cut into a 90° wedge shape to avoid vignetting the dispersed light on its way from the diffraction grating to the detector. The stop is external to the lens system and is positioned at the distance to the center of the diffraction grating.

The optical system was first optimized in single-pass using a 35 mm field. The merit function was defined to minimize the RMS spot sizes for several discrete wavelengths spanning 3900 to 6200Å, with preferential weight given to the 5000 to 6200Å range. Lateral color was allowed because it is of no significance once cross-dispersion is introduced. Spot diagrams for a single pass are shown in Figure 2.

Camera focus will initially be checked by taking calibration spectra while closing shutters that alternately block each half of the collimated light. In focus, spectral lines should show no discernable shifts. After a sufficiently large number of such focus tests at different instrumental temperatures, focus will be automatically adjusted by the focus actuator, triggered by measured instrumental temperature changes. Periodic manual checks using the above described shutter method will be performed as a "sanity check".

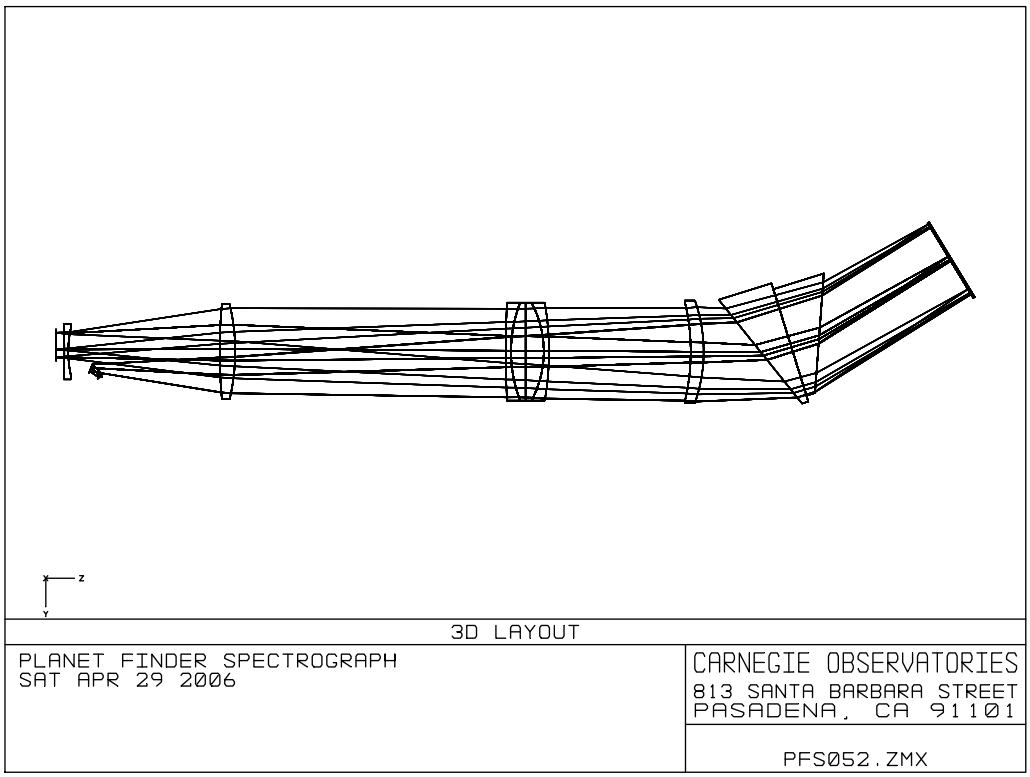

Figure 1. Optical layout of the PFS. The optical path shown begins at the fold mirrors that follow the silica lens wedge after the slit. Three wavelengths are shown: 4000, 5000, and 6000 Å.

2.2. Pre-slit Optics

The pre-slit optical layout (Fig. 3) serves several functions including focal reduction, target acquisition, active guiding, active telescope focusing, and injection of calibration lamp light.

The diverging F/11 telescope light is collimated by an off-the-shelf achromatic doublet lens. It is then refocused at F/5 using two doublets, one of which is off-the-shelf and one that is a combination of a custom and an off-the-shelf lens.

After the telescope light is collimated, it encounters a beamsplitter that transmits roughly 90% of the light. The transmitted light gets focused at F/5 to the position of the reflective slit, and then bounces back where it is recollimated. When the reflected light encounters the beamsplitter again, about 10% reflects upward toward the guide camera.[4] It is refocused at F/11 so that the guide camera has an effective plate scale equal to that of the telescope. The field of view on the 1024^2 13μm pixel EEV CCD is about 38×38 arcsec. Upon target identification, the star can be centered on the slit.

The remaining 10% of the light that is reflected on the first encounter with the beamsplitter will be directed to two butted, plane mirrors that are each slightly ($\sim$1 arcmin) angled with respect to the optical axis. Since these mirrors are in the collimated beam, this effectively slices the pupil into two halves. The reflected light passes through the beamsplitter and the pupil halves are focused onto the guider CCD to either side of the central image of the star on the slit. If the star begins to wander off of the slit, the images of the pupil halves will translate together in the opposite direction of the wandering slit image (Fig. 4). The two pupil half images also carry telescope focus information. As the telescope moves through focus on the slit, the directional senses of the pupil halves change. The measured centroids of their positions should stay a constant distance away from each other and the central slit image. If this distance changes, it betrays a wandering focus that can be automatically

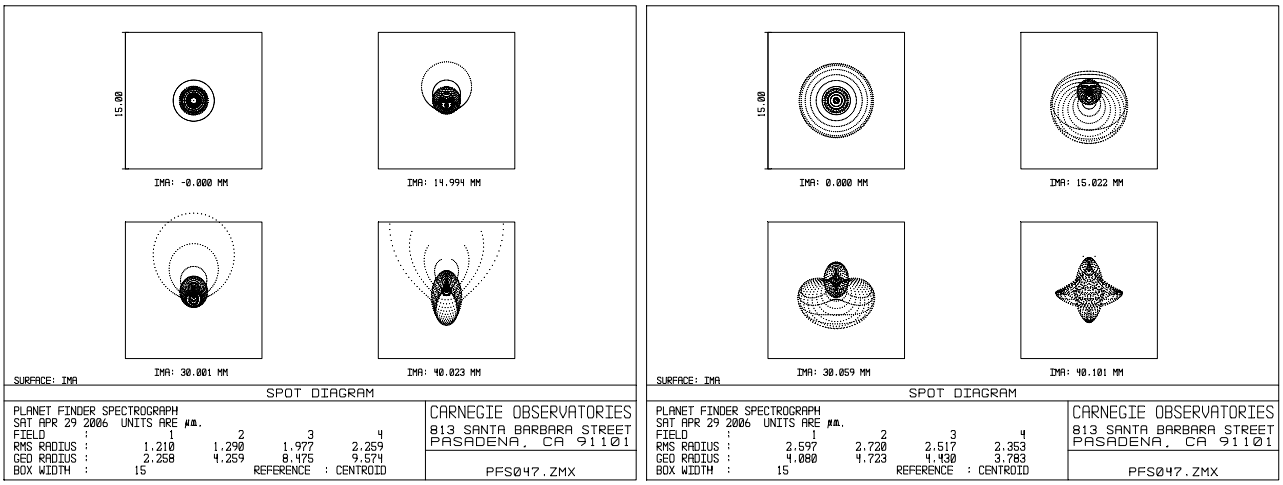

Figure 2. Spot diagrams of a single pass through the camera. Four field positions are shown each for 5000 Å (left) and 6200 Å (right). The 15μm boxes are repesentative of a single CCD pixel.

adjusted. It is expected that closely monitoring the positions of the pupil half images will be an effective way of precisely guiding and focusing the telescope to keep slit illumination even.

2.3. Slit and fold mirrors

The PFS will not rotate about the optical axis as the telescope moves. Since the instrument does not include an atmospheric dispersion corrector, the slit position angle on the sky will be set to 45° to optimize for minimal

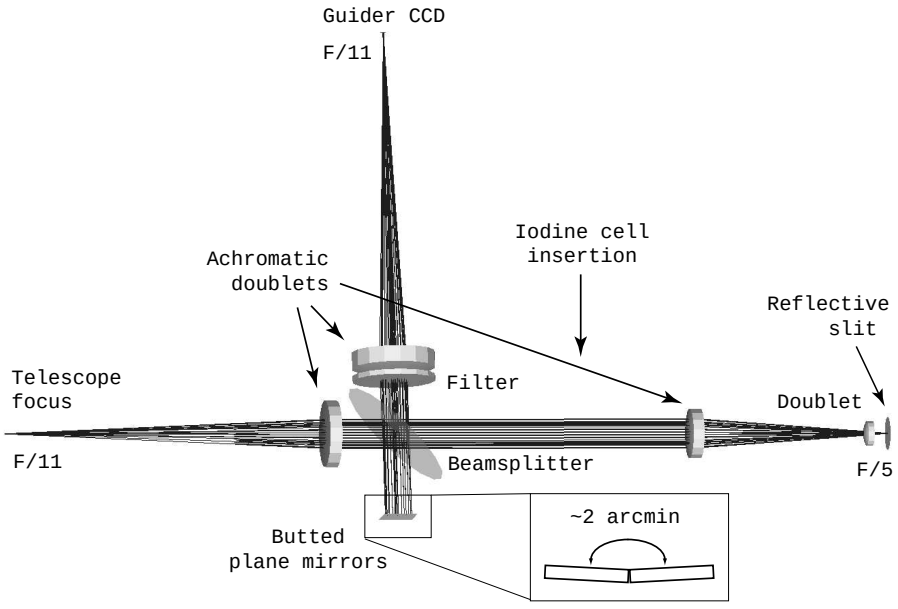

Figure 3. Pre-slit optical layout. F/11 telescope light is reduced to F/5 at the slit. Target acquisition may be accomplished along with active guiding and telescope focusing.

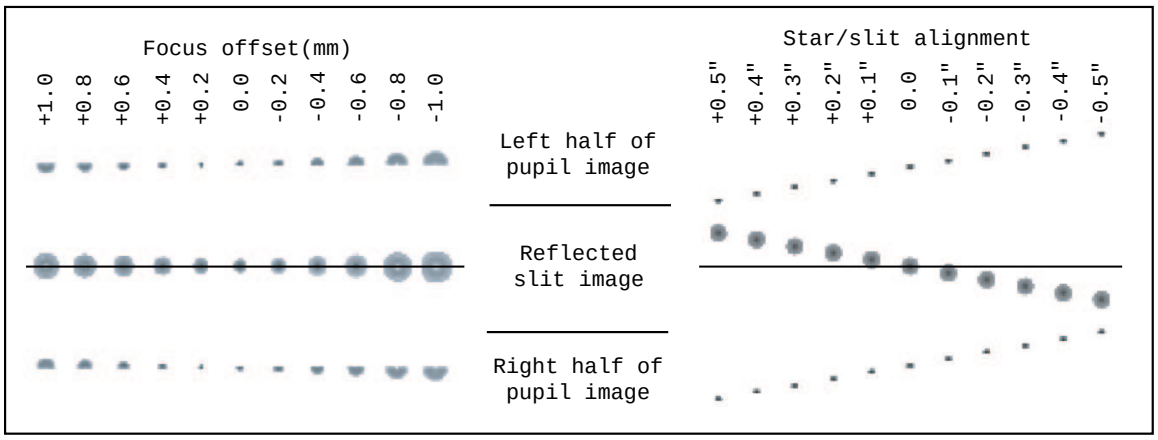

Figure 4. Simulated guide camera view of a target star under different focus and centering conditions. The centroids of the top and bottom pupil halves shift relative to center as the slit focus changes across the left sequence. The right sequence shows that the centering of the pupil halves shifts relative to the position of the star as slit centering changes.

atmospheric dispersion over a wide range of hour angles.

The optical axis of the spectrograph camera is slightly (1.51°) inclined relative to the telescope's optical axis because it is offset 30mm from center. This angle and the 45° degree slit position angle conspire to necessitate odd rotations of the optics with respect to the nasmyth platorm, which makes table-mounting difficult. To correct this, two fold mirrors will be mounted just past the wedge-shaped silica lens to effectively derotate the optical axis, positioning it parallel to the nasmyth platform and 90° off from the telescope's axis. The instrument also fits on the platform better in this orientation.

2.4. Dispersers

The primary dispersing element is a replicated R4 echelle grating from Richardson Grating Laboratory. Its ruled area is 154×408 mm. Despite being the longest standard echelle length available, illuminating the 76° blaze near true Littrow necessitates overfilling the grating and accepting a loss of efficiency. However, the alternative is to mosaic two such gratings, an expensive and unpleasant task. The extended spectral range of interest, 3900-6200Å, spans orders 99 to 157 while the primary wavelength range, 5000-6200Å, spans orders 99 to 123. The free spectral range of the reddest order is about 60.7 mm wide, which just fits on the 4096^2 15μm pixel CCD.

Cross-dispersion will be provided by two prism halves made of Ohara PBM2 glass. These will be bonded together to form a single prism with apex angle 43°. The total cross-dispersion spans 55.6 mm in the image plane, which allows enough room for time delay integration (Sect. 4) over several hundred rows. The minimum order separation is 4.0 arcsec. The echelle format is shown in Figure 5.

The cross-dispersion is oriented perpendicular to the top of the optical table (Sec. 3.1) in order to minimize any bi-planar differential expansion that might occur as a result of small thermal differences between the upper and lower optical table face sheets.

A consequence of placing the cross-dispersing prism before the grating in the optical path is that the angle of the slit image varies with wavelength across the orders. To minimize this effect, the slit will be rotated about 7° in order to align the slit image vertically at about 5600Å.

Changes in atmospheric temperature and pressure give rise to spectral shifts due to the changing refractive index of air. The effect is most serious in the collimated light near the grating. To alleviate this part of the local atmospheric effect, the grating will be enclosed in a vacuum chamber. An advantage of splitting the prism into two halves is that the interface between them provides a flat, circular surface that can easily be used as a vacuum

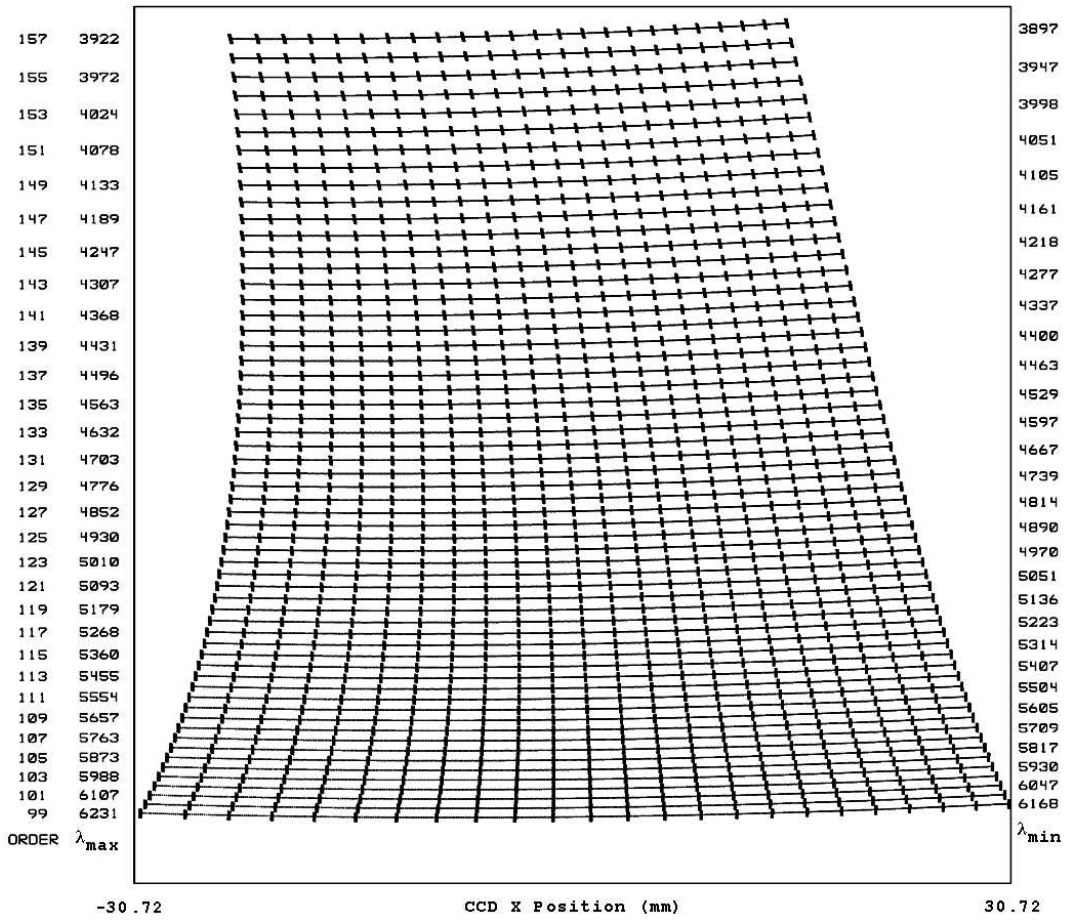

Figure 5. Echelle format. The free spectral range of each order is represented by a line. Images of a 0.7×3.7 arcsec slit are shown for discrete wavelengths to illustrate the wavelength-dependent line tilt.

window. An additional advantage is that both halves can be cut from a single piece of glass with roughly half the base length of the final prism.

The product of slit width and the PFS resolution is 38,000. With excellent camera optics and a spatial scale of about 0.1 arcsec/pixel, a minimum 0.2 arcsec slit can be used for a maximum resolving power of 190,000. In practice, however, it is expected that slit widths of 0.5-0.7 arcsec will be used for the planet search, yielding resolutions of 54,000-76,000.

2.5. Optical Fabrication

The stock optics used in the focal reducer were supplied by Edmund Optics and Optosigma. The custom lenses and prisms were figured and polished by Harold Johnson Optical Labs. The optical design was constrained to use only curvatures available in the HJOL test plate listing. All optics were figured to specification. Antireflection coatings were applied to all external surfaces with the exception of the front face of the first prism half (Sec. 4). The coatings were applied by ZC&R Coatings for Optics and are basically extended ultraviolet versions of their stock BBAR BARC-5 coating. The quoted transmission is greater than 99.5% over the full 3900-6200Å wavelength range.

The triplet and prism halves will be bonded with Sylgard 184, an optical RTV made by Dow Corning, in the

manner described by Bernstein et al.[3] The RTV thickness will be set to 0.003 inches between like glasses and to 0.009 inches between unlike glasses.

3. MECHANICAL DESIGN

A requirement of long-term, high precision radial velocity monitoring is that the data be directly comparable to each other over the course of many years. To a large extent, this is achieved by the clever application of sophisticated data calibration procedures. The fiducial calibration provided by the iodine absorption lines is capable of homogenizing data in a highly repeatable manner. However, gains may be made by maximizing instrument stability so that there are fewer, and less significant, variable instrumental effects that need to be removed by calibration. Ideally, one would like to establish the instrument's location and maintain it precisely over time, actively stabilizing environmental conditions while physically disturbing it as little as possible. This is the approach used for ESO's HARPS[5] spectrograph, which is maintained in vacuum in a thermally controlled room and fed by fiber optics that transmit light from the telescope. The PFS will not be fiber-fed, however, and therefore must be directly mated to the telescope.

When in use, PFS will be positioned on the nasmyth platform of the Clay telescope. When not in use, it must be removed from the platform since other instruments share the same telescope focus. It therefore must be mobile, but reproducibly mountable in order to maximize long-term stability.

3.1. Structure

PFS is shown in Figures 6 and 7. The instrument cart is a structural steel frame with three hard mount points. Base plates for the mount points will be welded to the nasmyth platform during instrument commissioning. These receive mounting blocks that hold hardware to provide a fully kinematic mount that should in turn yield highly repeatable instrument positioning relative to the telescope focal plane each time instrument changes occur. When PFS is to be moved, shock-absorbing casters are lowered to the platform on jacks and so lift the instrument away from the hard mount points.

Thermal stability is desirable. In the absence of perfect thermal control and stability, however, the next best thing is to limit thermal changes and their effects to be be very slow, accurately monitored, and predictably repeatable. To dampen the effects of diurnal temperature changes, the PFS optical system will be enclosed in a volume surrounded by rigid polyurethane sandwiched and glued between $\frac{1}{32}$ inch anodized aluminum sheets totaling 8 inches thickness. It is estimated that typical diurnal temperature variations would then give rise to about 0.3°C internal instrumental variations. Longer-term, seasonal variations will of course cause larger instrumental temperature changes. The insulating enclosure attaches to the steel instrument frame and is kinematically decoupled from the optical system except through the common instrument cart. Wind buffeting should have minimal effect on the vibrational stability of the optics.

The optical system is mounted on a custom, super invar optical table that is held about 12 inches above the instrument cart by three G10 tubes. At the interface between the tubes and the bottom sheet of the optical table are steel flanges attached to blade flexures. Arranged 120° relative to each other, these flexures provide rigidity, but allow for differential thermal expansion between the steel frame (and nasmyth platform) and the invar table without any danger of stick/slip mechanical shocking.

3.2. Pre-slit Assembly

The pre-slit assembly includes the focal reducing optics, guide camera, iodine cell, and calibration lamps. The latter three are sources of heat that must be isolated from the rest of the instrument. The assembly is housed in an aluminum box that is attached to, but held away from, the optical table with two G10 "arms" (Fig. 7). The front surface of the box points toward the telescope and is flush with the exterior of the insulating enclosure. The back of the box is thermally shielded from the rest of the instrument using polyurethane insulation. Some of the focal reducing optics are exterior to the box, extending into the instrument enclosure to the slit. These are mounted in a tube attached to the box, but thermally isolated using a section of G10 tube.

The iodine cell will be temperature controlled to 50°C.[6] It will be mounted on a linear stage that includes three controlled positions, one of which is empty, and one of which holds a blank window with an optical path length matched to that of the iodine cell.

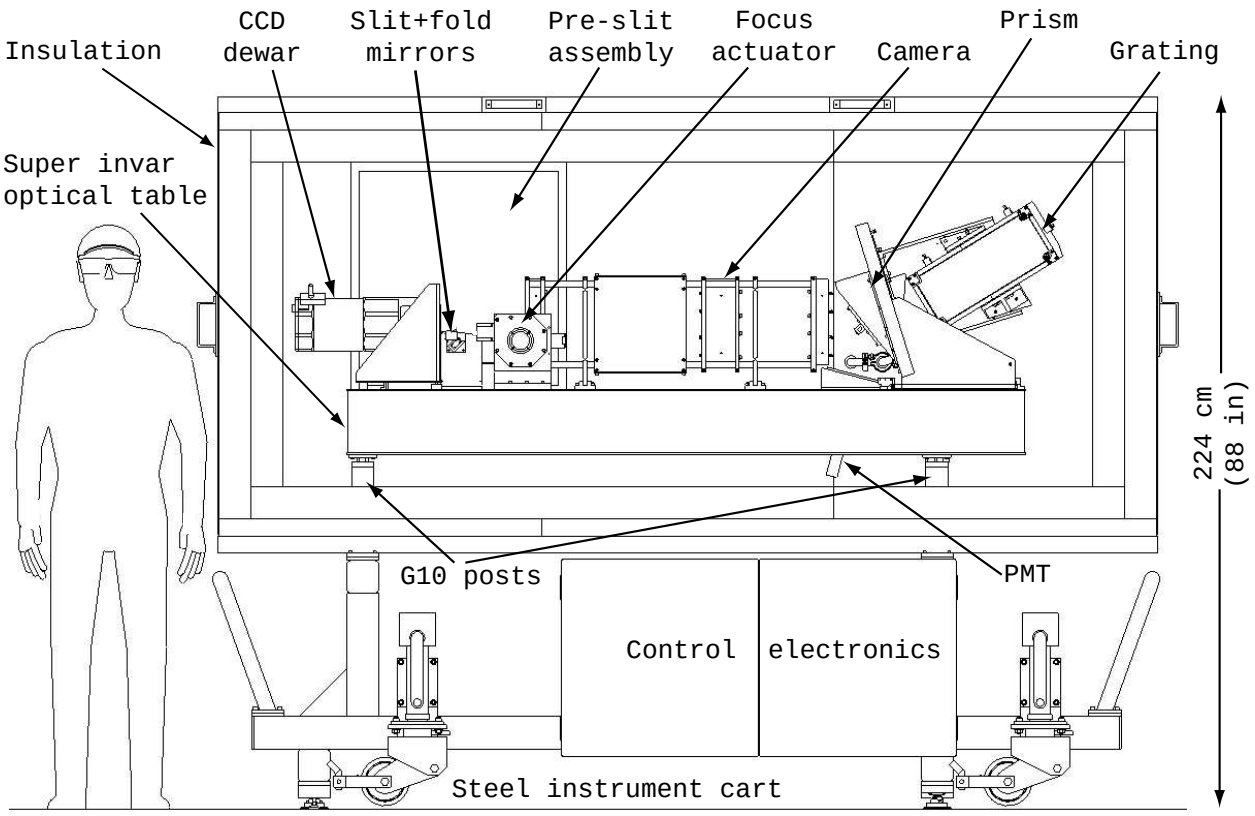

Figure 6. Side view of PFS, facing the telescope. The nearest side of the insulating enclosure has been removed for clarity, as has the shell that encloses the grating vacuum chamber.

3.3. Slit Assembly

The slit mask is a nickel-plated silicon wafer etched in a bi-metal process by Photo Sciences, Inc. One of several different slits may be selected by remotely operating a motor-driven linear stage. The slits are 3.7 arcsec long and vary in width from 0.2 to 3.0 arcsec. Normal operation will make use of either the 0.5 or 0.7 arcsec slit. A long slit is available for creating order-mixed flat field images. A pinhole is also available for creating more precise order-mapping frames.

Just behind the slit, a holographic diffuser may be inserted (remotely) into the beam to produce "milky" flats.

The instrument shutter sits just behind the holographic diffuser. It is a bi-stable leaf shutter manufactured to order by DACO Instrument Company. Power is required only to move the shutter to the open or closed position. Once in position, no power is required to hold the leaf in place, so heat dissipation is negligible.

Beyond the shutter is mounted the quartered silica lens that acts as a counterpart to the dewar window/field flattener. Just beyond this are mounted the two fold mirrors that effectively derotate the instrument's optical axis, fold the light perpendicular to the telescope's optical axis, and align the cross-dispersion perpendicular to the table top.

3.4. Camera Mount

The camera lenses are mounted in cells with one group to a lens cell. The lens cells are mechanically fixed relative to each other by four linear shafts, one at each corner. The lens cells include an inner and outer cell. The outer cell is fixed and the inner cell may be adjusted for lateral lens alignment. After initial alignment, the inner cell

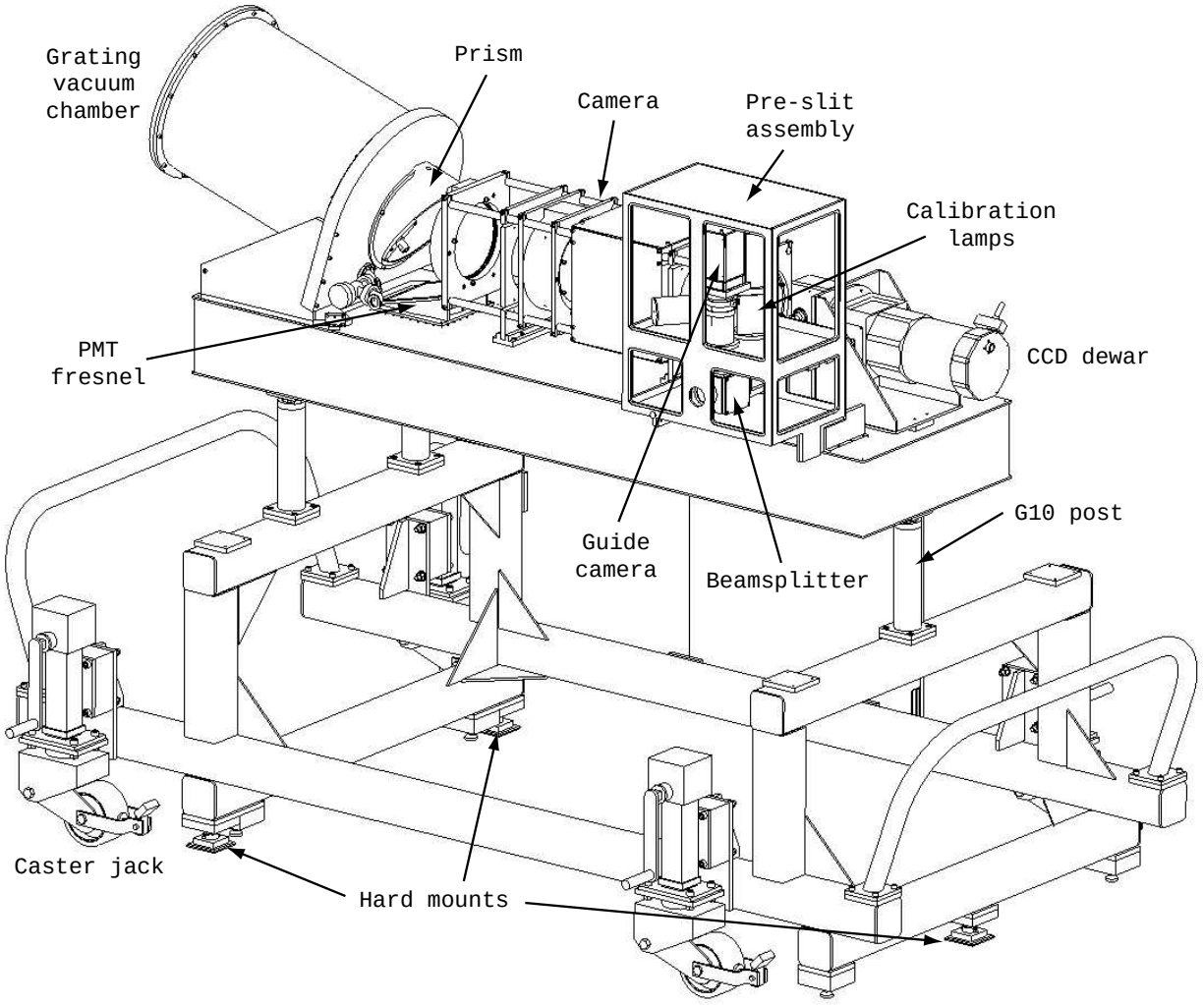

Figure 7. PFS viewed offset from the telescope's perspective. The insulating enclosure has been removed for clarity. Note that in this figure, the design of the pre-slit assembly (shown with its covers removed) and CCD dewar mount are preliminary.

positions are locked into place with screws. All glass contact is made through slightly compliant silicone rubber pads. Each inner cell features an annular retaining ring on one side, and a preload ring on the other. The preload ring is held in place with springs that apply 1.5G force axially to keep the lenses firmly seated. A radial spring preload is also applied to each lens group vertically from the top, with two additional radial pads 45° off from the bottom.

The full camera assembly is attached to the optical table through two blade flexures. An actuator pushes against one lens cell to bend the flexures and move the entire camera ±1 mm in order to adjust instrument focus as temperature changes.

3.5. Prism and Grating Mount

The echelle grating is mounted inside a vacuum vessel. The dependence of the refractive index of light on pressure has significance at the 86 m s^{-1} $mbar^{-1}$ level. In order to negate this effect at the 1 m s^{-1} level, the vacuum must be lower than about 10^{-2} mbar. Since active maintenance of a constant instrument temperature will not be employed, it will be advantageous to allow efficient thermalization. This sets the lower limit of the desirable

vacuum to $\sim 10^{-4}$ mbar, the pressure at which the mean free path of air equals the longest dimension of the vacuum chamber.

The first half of the prism is larger than the second half by 15 mm in diameter and acts as the vacuum window. The assembly is made entirely of aluminum, with the angled front plate (Fig. 6) acting as the base mount for all of the dispersing optics. Care was taken to choose the plate thickness to minimize variable atmospheric pressure-induced grating deflections that would give rise to spectral shifts and potential velocity errors. Finite element analyses showed that the grating rotation in the dispersion direction is essentially zero with a 1.7 inch thick plate. It is expected that a small, but noticeable shift in spectral position will occur when the vessel is pumped from atmospheric pressure down to $\sim 10^{-3}$ mbar, but this shift should be repeatable in the event that the vessel must be pressurized and depressurized multiple times. Under vacuum, external changes in atmospheric pressure will induce tiny deflections in the front plate, but these should be insignificant in the dispersion direction, and tiny in the cross-dispersion direction. They should also be repeatable, so that with careful automatic logging of atmospheric conditions during observing, any remaining instrumental effects can be removed.

4. DETECTORS

The detector is a SITe 4096×4096 CCD with 15μm pixels obtained from the University of Arizona Imaging Technology Laboratory. It will be housed in a custom head attached to an Infrared Labs liquid nitrogen dewar that will be filled from and vented to the outside of the PFS insulation enclosure.

At the 1 m s^{-1} precision level, tiny, sub-pixel inconsistencies can have a detrimental effect on measurement accuracy. To combat this, each PFS exposure will be taken using time delayed integration (TDI). The CCD will be physically panned in the cross-dispersion direction by mechanically pushing its flexure-mounted stage a distance equivalent to a few hundred CCD rows. By spreading the exposure over several hundred pixels for each wavelength, very flat, uniform responses can be expected for the full spectrum. Any sub-pixel variations will be washed out. The timing of the CCD panning and charge-shifting will be slave to the output of a photomultiplying tube (PMT) that will monitor a small amount of light reflected from the uncoated front surface of the prism.

The PMT will mount inside a hole that has been prepared in the custom optical table. In addition to providing feedback for the TDI, the output from the PMT can be used to determine the photon-weighted mean exposure time so that appropriate barycentric corrections can be made to the measured radial velocities. The PMT may also be used as a total exposure timer. Rather than specify an exposure time, the observer may choose to specify a desired signal to noise level and allow the software to operate the shutter when the PMT has counted enough photons.

5. STATUS

All PFS optics have been figured, polished, and coated. Machining is progressing rapidly. Complete laboratory assembly is expected by early fall 2006. Instrument commissioning at Las Campanas Observatory is expected by summer 2007, with science operations following shortly thereafter.

ACKNOWLEDGMENTS

We thank Greg Burley, Steve Gunnels, Matt Johns, Frank Perez, Ian Thompson and Alan Uomoto for valuable discussions. This work was supported by the National Science Foundation under award number AST-0116529, a generous gift from Mr. Frank H. Pearl, and the Carnegie Institution of Washington.

REFERENCES

1. G. W. Marcy and R. P. Butler, "Precision radial velocities with an iodine absorption cell," *PASP* **104**, pp. 270–277, 1992.
2. H. Dekker, S. D'Odorico, A. Kaufer, B. Delabre, and H. Kotzlowski, "Design, construction, and performance of uves, the echelle spectrograph for the ut2 kueyen telescope at the eso paranal observatory," in *Optical and IR Telescope Instrumentation and Detectors*, M. Iye and A. F. Moorwood, eds., *Proc. SPIE* **4008**, pp. 534–545, 2000.

3. R. Bernstein, S. A. Shectman, S. M. Gunnels, S. Mochnacki, and A. E. Athey, "Mike: A double echelle spectrograph for the magellan telescopes at las campanas observatory," in *Instrument Design and Performance for Optical/Infrared Ground-based Telescopes*, M. Iye and A. F. Moorwood, eds., *Proc. SPIE* **4841**, pp. 1694–1704, 2003.
4. G. Burley, I. Thompson, and C. Hull, "Compact ccd guider camera for magellan," in *Scientific Detectors for Astronomy, The Beginning of a New Era*, P. Amico, J. W. Beletic, and J. E. Belectic, eds., pp. 431–434, 2004.
5. F. Pepe, M. Mayor, B. Delabre, D. Kohler, D. Lacroix, D. Queloz, S. Udry, W. Benz, J. L. Bertaux, and J. P. Sivan, "Harps: a new high-resolution spectrograph for the search of extrasolar planets," in *Optical and IR Telescope Instrumentation and Detectors*, M. Iye and A. F. Moorwood, eds., *Proc. SPIE* **4008**, pp. 582–592, 2000.
6. R. P. Butler, G. W. Marcy, E. Williams, C. McCarthy, P. Dosanjh, and S. S. Vogt, "Attaining doppler precision of 3 m/s," *PASP* **108**, p. 500, June 1996.